

Final report for PD124380: Correlation and finite-temperature effects in metallic magnets

Principal investigator: András Deák

1 Research background

Our research concerns the magnetism of heterostructures and bulk systems important for the purposes of potential spintronics applications. In particular, we focus on materials with non-trivial anisotropy effects, electronic correlations and complex spin textures.

We use the Screened Korrington–Kohn–Rostoker (SKKR) Green’s function technique to compute the electronic structure of crystalline systems. The method is designed to be performant and accurate for structures with only two-dimensional translation invariance (surfaces and interfaces), but it can also be applied to bulk systems. After self-consistent calculations we can perform calculations to extract spin models from the electronic structure, enabling multiscale approaches building from the *ab initio* level.

In the present final report we will list our research findings and the progress of the three-year research project.

2 Superconductivity and magnetism in heterostructures

We investigated electronic correlations of a different kind as compared to the primary target of the research project in a study of *ab initio* superconductivity, performed in a broader theoretical collaboration. We started developing a fully relativistic spin-polarized multiple-scattering theory for inhomogeneous superconductors which can also be applied to superconducting/normal-metal/ferromagnet heterostructures. The method uses a semiphenomenological parametrization of the exchange-correlation functional to solve the first-principles Dirac–Bogoliubov–de Gennes equations. Care has to be taken in the cases where left-hand-side and right-hand-side solutions to the equations differ. We applied the theory to Nb/Fe and Nb/Au/Fe heterostructures. We found Fulde–Ferrell–Larkin–Ovchinnikov-like oscillations in the iron layers, but more interestingly an oscillatory behavior is observed in the gold layers as well. The band-structure calculations suggest that this is the consequence of an interplay between the quantum-well states in the interface and ferromagnetism of the iron bulk. Our work was published in Physical Review B [1].

3 Multiscale study of magnetic heterostructures

Fe/MgO-based magnetic tunnel junctions are promising candidates for spintronic devices due to their high thermal stability and high tunneling magnetoresistance. We performed a fully relativistic multiscale study of MgO/Fe/MgO sandwiches using first-principles calculations and atomistic spin modeling. Frustrated exchange interactions at the Fe/MgO interfaces lead to the emergence of spin spirals at the interfaces, despite an overall ferromagnetic ground state of the Fe slab. The frustration at the interface destabilizes the magnetization at higher temperatures, thereby reducing the Curie temperature. We found a large contribution to the effective interfacial magnetic anisotropy from the two-ion exchange energy, which dominates the on-site anisotropy (see Fig. 1). The different temperature dependence of the interface and bulk-like anisotropies ultimately leads to an unexpected non-monotonic temperature variation of the effective magnetic anisotropy energy. We published our findings in Physical Review Applied [2].

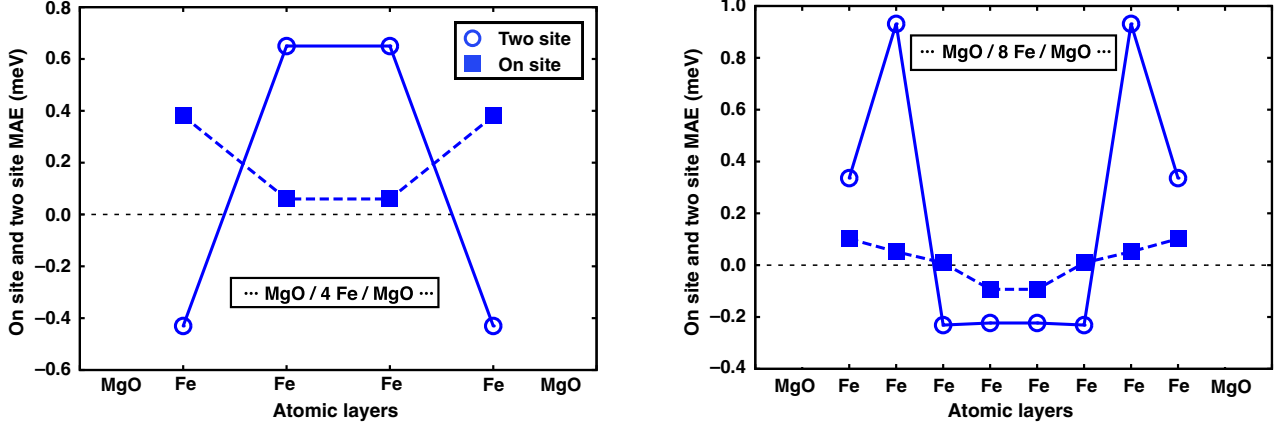


Figure 1: Two-site and on-site anisotropy contributions in $\text{MgO}/n\text{Fe}/\text{MgO}$ for $n = 4$ (left) and $n = 8$ (right). The two-site contributions dominate the anisotropy, and especially contributions from the interfaces of the Fe slab. The strong layer dependence of the magnetic interactions eventually leads to a curious non-monotonic temperature dependence of the effective anisotropy. (Figure taken from Ref. 2)

4 Non-collinear spin textures

4.1 Weyl semimetal Mn_3Sn

We joined into collaboration investigating the triangular antiferromagnet Mn_3Sn with focus on its magnon spectrum, providing a joint experimental and theoretical description. Mn_3Sn has recently attracted considerable attention as a magnetic Weyl semimetal exhibiting transport anomalies at room temperature. We reported the spin wave spectra measured with inelastic neutron scattering, and used linear spin wave theory to derive a suitable magnetic Hamiltonian. Supported by *ab initio* calculations, the Hamiltonian produces the expected helical ordering with $k_z = 0.0904$, consistent with the real ground state of this material. We investigated the influence of the Dzyaloshinskii–Moriya (DM) interaction on the spiral ordering, see Fig. 2. Our work provides a rare example of the intimate coupling between the electronic and spin degrees of freedom for a magnetic Weyl semimetal system. Our results were published in npj Quantum Materials [3].

4.2 Mn_3Z family of noncollinear antiferromagnets

Following our investigation of Mn_3Sn we turned to the exploration of weak ferromagnetism in Mn_3Sn and two related compounds, Mn_3Ge and Mn_3Ga . We set up a model based on three Mn sublattices based on spin model parameters computed from first-principles. We showed using a group theoretical argument that there are two degenerate (in-plane weakly ferromagnetic) ground states that arise as a superposition of a triangular state and a ferromagnetic (FM) state. We observed the ground state configuration of the classical spin models for each system, and derived analytical expressions for the weak ferromagnetic distortions. Finally, self-consistent fully relativistic calculations were performed to assess the weak ferromagnetic states directly on the *ab initio* level. Going beyond a spin model description enabled us to probe orbital moments in these materials, which curiously seem to follow a decomposition predicted by group theory. By selectively disabling the spin-orbit coupling on different sublattices, we traced how these site-resolved contributions affect the ground state and the weak ferromagnetic moment. We published our investigations in Physical Review B [4].

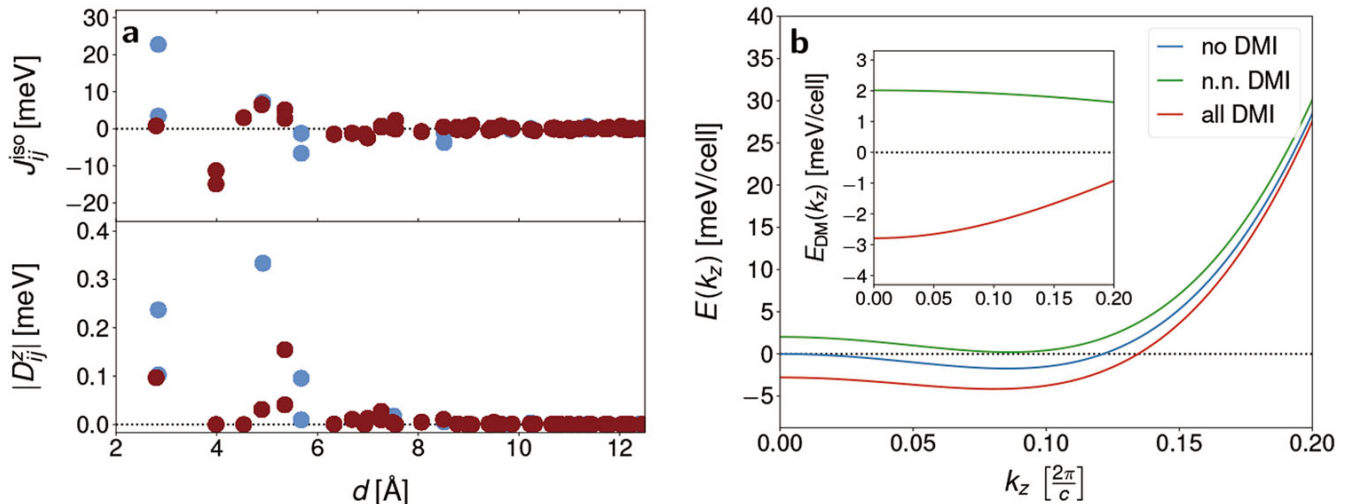


Figure 2: **a** isotropic Heisenberg coupling (top) and magnitude of DM z component (bottom) in Mn_3Sn . Red and blue circles denote out-of-plane and in-plane couplings, respectively. **b** Spin spiral energy from the spin model, using only isotropic terms (blue curve), first nearest neighbour DM couplings (green curve) and the full spin model (red curve). The inset shows the DM energy contribution alone. It is evident that the system cannot be described by nearest-neighbour DM interactions, as both the location of the energy minimum and the depth of the minimum are affected by farther neighbours. (Figure taken from Ref. [3])

5 Computational developments

5.1 Exchange interactions from nonorthogonal basis sets

Following the strategy of deriving spin models for magnetically ordered systems using KKR, we presented a computational scheme to determine the exchange parameters of isotropic spin models applicable to density functional methods that are based on nonorthogonal basis sets. We integrated the technique in the SIESTA code and demonstrated that its output reproduces the Heisenberg interactions of simple metallic bulk ferromagnets as obtained from well-established computational approaches. We also applied the method to two-dimensional materials with sp magnetism, namely graphene nanostructures. For fluorinated graphene we obtained exchange interactions in fairly good agreement with previous calculations using maximally localized Wannier functions and we confirmed the theoretical prediction of a 120° Néel state. Associated with the magnetic edge states of a zigzag graphene nanoribbon we found rapidly decaying exchange interactions, however with an unconventional distance dependence of $e^{-\sqrt{r/\delta}}$. We showed that the stiffness constant derived from the exchange interactions is consistent with a previous estimate based on total energy differences of twisted spin configurations. Our findings were published in Physical Review B [5].

5.2 Improved bulk performance for SKKR

We also spent time developing our SKKR implementation in ways that do not directly translate to publications, but instead make our subsequent research more efficient. In particular, we have added a three-dimensional bulk implementation to both the self-consistent and spin model calculation codes, and implemented the LSDA+U method for computing exchange interactions.

Since the SKKR method is designed for use with systems with two-dimensional translation invariance (surfaces and interfaces), its implementation contains two-dimensional Brillouin zone integrations, and the “perpendicular” direction is preserved in real space. Thanks to the Green’s function technique we can calculate surface Green’s functions for the two real-space terminals of the simulated system, thereby defining boundary conditions that implement exactly infinite crystals (or vacuum) on two sides of the region of interest. The advantage of this approach is that heterostructures and surfaces can be computed exactly in the sense that the two bulk terminals are treated as truly infinite regions. This is in strong contrast to most electronic structure codes, which rely on three-dimensional translation invariance

and consequently have to approximate layered non-bulk systems with large supercells. This traditional approach can be less efficient, and it distorts the electronic structure by introducing spurious three-dimensional periodicity.

The trade-off of our accuracy for layered systems is that calculations for bulk systems are slower and need more memory than would be possible with a fully bulk code. In order to reduce some of this cost we have implemented a three-dimensional bulk option in our SKKR program, which makes it possible to utilize a three-dimensional Brillouin zone integral. Due to details of the implementation this is primarily useful for bulk systems with large unit cells, but in this case both calculation time and memory need can be drastically reduced with the new calculation mode. A significant consequence of the development is that our code can now compute band structure “spaghetti” plots, see Fig. 3 for the band structure of bcc Fe as an example.

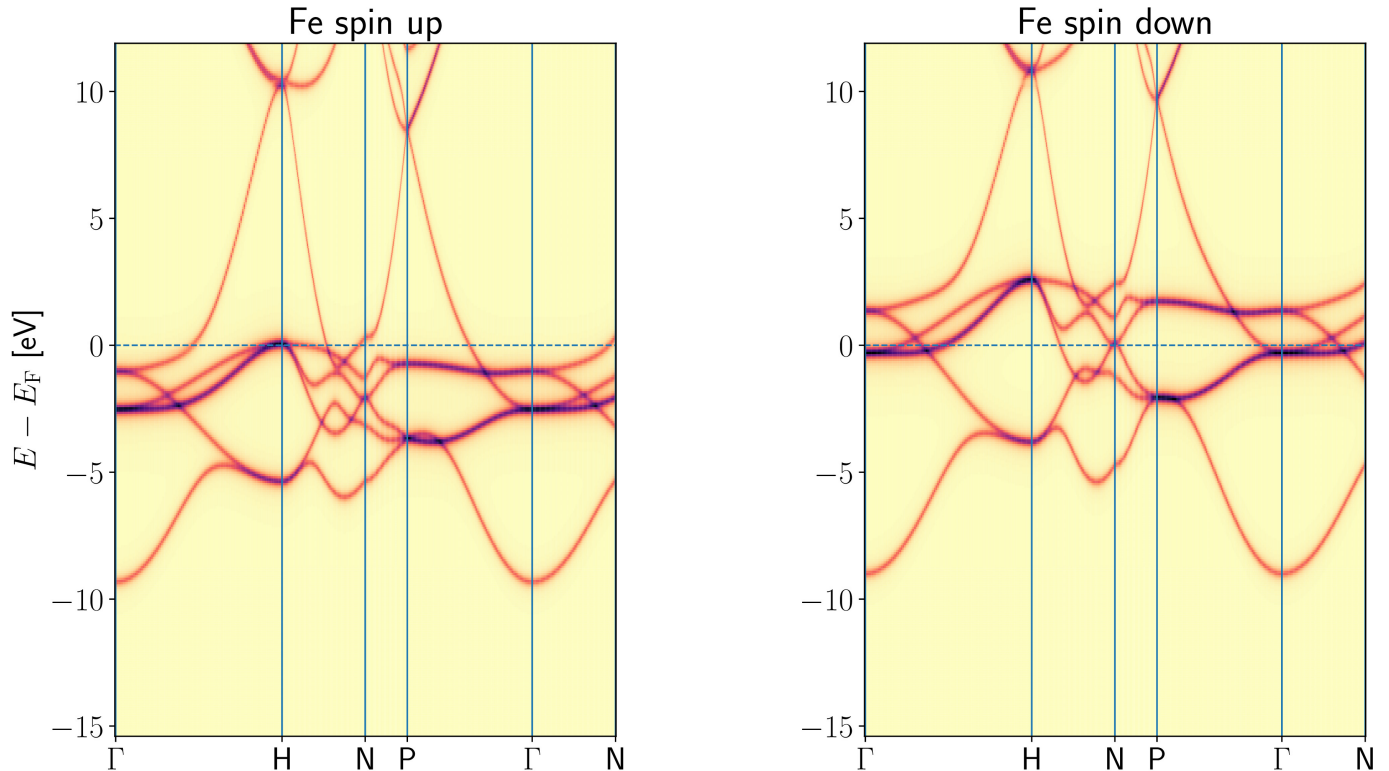


Figure 3: Bulk band structure of bcc Fe. The construction of this figure was made possible by the new bulk mode of our SKKR program.

It is fairly straightforward to extend the same bulk treatment to our programs that compute spin model parameters, which in practice makes it possible to include arbitrarily distant interactions without having to increase the size of the simulated region. This is again especially useful for bulk systems with large unit cells, since a single large unit cell can be used to compute a full suite of couplings in a spin model, thereby reducing memory need and runtime for our calculations.

6 Ongoing investigations

6.1 Hematite

We have started investigations of hematite (α - Fe_2O_3), the subject of the original investigations of Dzyaloshinskii [6] and Moriya [7]. This insulating antiferromagnet has gathered current attention for possible uses in spin transport applications [8].

The hexagonal unit cell of hematite contains 30 atoms. The new three-dimensional bulk option has made it possible to reduce the memory and runtime need of our calculations targeting this system. Self-consistent calculations have revealed that the GGA+U approximation is necessary in order to obtain realistic sizes for the band gap and

magnetic moment. *Ab initio* band energy calculations verify that the perpendicular antiferromagnetic (AFM) state is by around $10 \mu\text{Ry}/\text{Fe}$ atom lower in energy than the in-plane one, a necessary condition for the Morin transition [9] to occur at finite temperature. We see a weak ferromagnetic distortion of the in-plane AFM state with 0.03° distortion angle, in excellent agreement with earlier theoretical investigations [10].

We are currently in the process of computing spin model parameters for hematite. The new implementation of both the LDA+U approximation and the three-dimensional bulk mode has made these calculations feasible. Preliminary results are promising, as the spin model obtained from the electronic structure is consistent with an AFM ground state with a Néel temperature close to that of hematite. Further plans include investigating finite-temperature behaviour to assess the presence of the Morin transition, and its dependence on spin model parameters (notably, the strength of the Dzyaloshinskii–Moriya interaction and the uniaxial anisotropy).

6.2 CrB₂

We are also investigating the magnetic properties of bulk CrB₂, a metallic triangular antiferromagnet that has gained recent interest for studying magnonics in non-collinear spin structures [11]. Containing triangular layers of Cr separated by honeycomb layers of B, its magnetism seems to result from the delicate interplay of various effects. A Cr magnetic moment of realistic size can only be stabilized by going beyond the local spin-density approximation, and subtle details of the calculations such as the choice of atomic radii to which results are normally not sensitive to, seem to matter.

Following self-consistent field calculations performed in both the FM and paramagnetic states, we derived exchange interactions. Mean-field estimates suggest that the ground state of the system is an incommensurate spin spiral with modulation vector pointing along nearest-neighbour Cr pairs, in agreement with experiment [12]. A careful numerical analysis of the mean-field Néel temperature and the corresponding modulation vector of the mean-field ground state estimate shows that extremely distant exchange interactions (up to 5 lattice constant units) affect magnetic ordering, further demonstrating the delicate balance shaping the overall magnetic behaviour of this compound. We plan to perform Landau–Lifshitz–Gilbert spin dynamics and Monte Carlo simulations to investigate the true ground state of the obtained spin models, and to obtain a realistic (that is, non mean-field) temperature scale.

References

- [1] G. Csire, **A. Deák**, B. Nyári, H. Ebert, J. F. Annett, B. Újfalussy, *Phys. Rev. B* **97**, 024514 (2018)
- [2] R. Cuadrado, L. Oroszlány, **A. Deák**, T. A. Ostler, A. Meo, R. V. Chepulskii, D. Apalkov, R. F. L. Evans, L. Szunyogh, R. W. Chantrell, *Phys. Rev. Appl.* **9**, 054048 (2018)
- [3] P. Park, J. Oh, K. Uhlřřová, J. Jackson, **A. Deák**, L. Szunyogh, K. H. Lee, H. Cho, H.-L. Kim, H. C. Walker, D. Adroja, V. Sechovský, J.-G. Park, *npj Quant. Mats.* **3**, 63 (2018)
- [4] B. Nyári, **A. Deák**, and L. Szunyogh, *Phys. Rev. B* **100**, 144412 (2019)
- [5] L. Oroszlány, J. Ferrer, **A. Deák**, L. Udvardi, L. Szunyogh, *Phys. Rev. B* **99**, 224412 (2019)
- [6] I. Dzyaloshinsky, *J. Phys. Chem. Solids* **4**, 241 (1958)
- [7] T. Moriya, *Phys. Rev.* **120**, 91 (1960)
- [8] R. Lebrun, A. Ross, S. A. Bender, A. Qaiumzadeh, L. Baldrati, J. Cramer, A. Brataas, R. A. Duine, M. Kläui, *Nature* **561**, 222 (2018)
- [9] F. J. Morin, *Phys. Rev.* **78**, 819 (1950)
- [10] V. V. Mazurenko, V. I. Anisimov, *Phys. Rev. B* **71**, 184434 (2005)
- [11] P. Park, K. Park, T. Kim, Y. Kousaka, K. H. Lee, T. G. Perring, J. Jeong, U. Stuhr, J. Akimitsu, M. Kenzelmann, J.-G. Park, *Phys. Rev. Lett.* **125**, 027202 (2020)

[12] S. Funahashi, Y. Hamaguchi, T. Tanaka, E. Bannai, *Solid State Commun.* **23**, 859 (1977)